Robust $N-k$ Security-constrained Optimal Power Flow Incorporating Preventive and Corrective Generation Dispatch to Improve Power System Reliability

Liping Huang, *Student Member*, *IEEE*, Chun Sing Lai, *Senior Member*, *IEEE*, Zhuoli Zhao, *Member*, *IEEE*, Guangya Yang, *Senior Member*, *IEEE*, Bang Zhong, and Loi Lei Lai, *Life Fellow*, *IEEE*

***Abstract*—As extreme weather events have become more frequent in recent years, improving the resilience and reliability of power systems has become an important area of concern. In this paper, a robust preventive-corrective security-constrained optimal power flow (RO-PCSCOPF) model is proposed to improve power system reliability under $N-k$ outages. Both the short-term emergency limit (STL) and the long-term operating limit (LTL) of the post-contingency power flow on the branch are considered. Compared with the existing robust corrective SCOPF model that only considers STL or LTL, the proposed RO-PCSCOPF model can achieve a more reliable generation dispatch solution. In addition, this paper also summarizes and compares the solution methods for solving the $N-k$ SCOPF problem. The computational efficiency of the classical Benders decomposition (BD) method, robust optimization (RO) method, and line outage distribution factor (LODF) method are investigated on the IEEE 24-bus Reliability Test System and 118-bus system. Simulation results show that the BD method has the worst computation performance. The RO method and the LODF method have comparable performance. However, the LODF method can only be used for the preventive SCOPF and not for the corrective SCOPF. The RO method can be used for both.**

***Index Terms*—Benders cut, bender decomposition, line outage distribution factor, $N-k$ security criterion, optimal power flow, power system reliability, resilience, robust optimization.**

Manuscript received September 1, 2021; revised November 25, 2021; accepted January 12, 2022. Date of online publication May 6, 2022, date of current version June 18, 2022. This work was supported by the Education Department of Guangdong Province: New and Integrated Energy System Theory and Technology Research Group (No. 2016KCXTD022); National Natural Science Foundation of China (No. 51907031); Guangdong Basic and Applied Basic Research Foundation (Guangdong-Guangxi Joint Foundation) (No. 2021A1515410009); China Scholarship Council; Brunel University London BRIEF Funding.

L. P. Huang, Z. L. Zhao and L. L. Lai are with the School of Automation, Guangdong University of Technology, Guangzhou 510006, China.

C. S. Lai (corresponding author, email: chunsing.lai@brunel.ac.uk) is with the School of Automation, Guangdong University of Technology, Guangzhou 510006, China, and also with the Department of Electronic and Electrical Engineering, Brunel University London, London, UB8 3PH, UK.

G. Y. Yang is with the Center for Electric Power System and Energy, Department of Electrical Engineering, Technical University of Denmark, Kongens Lyngby 2800, Demark.

B. Zhong is with Zhaoqing Power Supply Bureau, Guangdong Power Grid Company, China Southern Power Grid, Zhaoqing 526020, China.

DOI: 10.17775/CSEEJPES.2021.06560

NOMENCLATURE

A. Sets and Indices

i, l, b, s	Indices of generators, transmission lines, buses, and the segments of piecewise linear production cost function.
$S_{\mathrm{G}}, S_L, S_{\mathrm{B}}, S_{\mathrm{S}}$	Sets of generators, transmission lines, buses, and the segments of piecewise linear production cost function.

B. Variables

F_i	The linearized production cost of generator i.
$F_{i,s}$	The linearized production cost of generator i on segment s.
$P_{\mathrm{G},i}$	The active power output of generator i before the outage.
$P_{\mathrm{LS},b}$	The planned load shedding at bus b before the outage.
$P_{\mathrm{L},l}$	The active power flow on line l before the outage.
$\theta_{s_l}, \theta_{e_l}$	The voltage angles of the source bus and the end bus of line l before the outage.
$\theta_{\mathrm{b}}, \theta_{\mathrm{ref}}$	The voltage angles of bus b and the reference bus before the outage.
$P_{\mathrm{b}}^{+}, P_{\mathrm{b}}^{-}$	The slack variables of the power balance constraint of bus b, which are used to indicate security violations after the outage.
ω	The objective of the feasibility check subproblem.
$P_{\mathrm{G},i}^{c}$	The active power output of generator unit i after the outage.
$P_{\mathrm{L},l}^{c}$	The active power flow on line l after the outage.
$\theta_{s_l}^{c}, \theta_{e_l}^{c}$	The voltage angles of the source bus and the end bus of line l after the outage.
$\theta_{\mathrm{b}}^{c}, \theta_{\mathrm{ref}}^{c}$	The voltage angles of bus b and the reference bus after the outage.
J_l^c	A binary variable used in the **SEP, SEP1 SEP2** problems to represent the status of line l (1 normal, 0 outage).
y_l	The auxiliary variable used in the single commodity flow method.
$\alpha, \beta, \gamma, \lambda, \delta, \chi, \sigma$	The dual variables of the constraints of the feasibility check problem.

μ	The auxiliary variables used to linearize the bilinear terms in the **SEP**, **SEP1**, and **SEP2** problems.

C. Constants and Parameters

NG	The total number of generators.
NB	The total number of buses.
N	The total number of transmission lines.
NS	The total number of the segments of the piecewise linear production cost function.
k	The maximum outage number of lines.
d_{b}	The cost coefficient of the planned load shedding at bus b.
$m_{i,s}, n_{i,s}$	Coefficients of the piecewise linear production cost function of generator i.
$A_{b,i}, K_{b,l}$	Elements of the bus-generator incidence matrix A and the bus-line incidence matrix K.
$P_{\mathrm{D},b}$	The active power demand at bus b.
x_l	The reactance of transmission line l.
$\theta_{\min,b}, \theta_{\max,b}$	The minimum and maximum voltage angles of bus b.
$P_{\mathrm{Gmin},i}, P_{\mathrm{Gmax},i}$	The minimum and maximum active power output of generator i.
$R_{\mathrm{D},i}, R_{\mathrm{U},i}$	The ramping up and ramping down limit of generator i.
$P_{\mathrm{Lmax},l}$	The power flow limit of transmission line l before the outage.
J_l^c	A parameter used in the SP problem indicating the status of line l (1 normal, 0 outage).
η	A parameter that defines how much the post-contingency power flow limit can be relaxed from the pre-contingency limit $P_{\mathrm{Lmax},l}$.
STL	A parameter that defines how much the post-contingency power flow limit can be relaxed from the pre-contingency limit $P_{\mathrm{Lmax},l}$ for a short-term time period after the outage, e.g., 120%.
LTL	A parameter that defines how much the post-contingency power flow limit can be relaxed from the pre-contingency limit $P_{\mathrm{Lmax},l}$ for a long-term time period after the outage, e.g., 100%.
p_l	The outage probability of transmission line l.
p_{ct}	A predetermined threshold for the probability of a contingency occurring.
ΔP_i	Ramping limit of generator i.

I. Introduction

A. Background and Motivation

THE security-constrained optimal power flow (SCOPF) problem is one of the important optimization problems in power system operations [1], which is used to determine an optimal generation dispatch schedule to supply the system load. Operation constraints for normal and post-contingency states are included in the SCOPF problem. A contingency is defined as an event that removes one or more generators or transmission lines from the power system. The SCOPF problem seeks an optimal solution that is feasible in any pre-specified possible contingency. A comprehensive review and discussion on the SCOPF problem can be found in [2] and [3].

In general, the SCOPF problem can be divided into three categories, namely the preventive SCOPF (PSCOPF) problem [4], the corrective SCOPF (CSCOPF) problem [5], and the preventive-corrective SCOPF (PCSCOPF) problem [6]. The PSCOPF problem aims to find an optimal preventive power dispatch solution that is secure in both normal and post-contingency states. Corrective actions are allowed in the CSCOPF problem to eliminate the security violation in the post-contingency state. In the PCSCOPF problem, both preventive and corrective control actions are used in the model, because not only the long-term operating limit (LTL) but also the short-term emergency limit (STL) on the branch are considered. Note that STL is larger than LTL, And both are necessary to answer the question of why it is important to consider both STL and LTL in the SCOPF problem. As we know, some transmission system operators may define several operating limits for a particular device, depending on the tolerable time frame for violation of the limits. For example, there are several limits on the current or power flow on a branch. Indeed, three power flow limits are defined in the French UHV network, i.e., the STL, the medium-term limits (MTL), and the LTL with delays of 1, 5, and 20 minutes for line disconnection [2]. The operating rules assume that the operator cannot react within one minute, so the STL must be met by preventive actions. Therefore, without considering the STL and preventive actions, as the CSCOPF problem does, the reliability of the resulting scheme is doubtful. We can indeed obtain the most reliable solution by considering the strictest LTL in the PSCOPF problem, but the production cost may be very high. Due to the long tolerable time for violation of the LTL, we can use corrective action to eliminate the violation, reducing generation costs. Therefore, considering both STL and LTL in the PCSCOPF problem and using different control actions to satisfy different operating limits can make the resulting scheduling scheme more practical and reliable.

Some research studies have addressed the PCSCOPF problem. However, most of the existing studies only focus on the $N-1$ security criterion or a small number of contingencies. For example, a PCSCOPF problem with $N-1$ security criterion was studied in [6] and [7]. A stochastic PCSCOPF problem considering outage probabilities of transmission lines was proposed in [8]. In [9] and [10], fast-response distributed battery energy storage was used as post-contingency corrective control actions to remove the violation of the STL. The $N-1$ contingency of transmission lines is investigated in various studies. Few existing studies have investigated the PCSCOPF problem with the $N-k$ security criterion, especially those based on robust optimization. However, $N-k$ outages are common during extreme events. As extreme weather events become more frequent in the future, this situation might become more severe. The PSCOPF and CSCOPF problems

with the $N-k$ security criterion have been studied by some authors [11] [12]. In this paper, an $N-k$ robust PCSCOPF (RO-PCSCOPF) is proposed.

As for the solution methods of the SCOPF problem, since there could be hundreds of components in a power system, the SCOPF problem may be computationally challenging because of the large number of contingencies. The problem is usually decomposed into an optimal power flow master problem and a set of feasibility check subproblems for each contingency. Solution methods based on Benders decomposition (BD), robust optimization (RO), and line outage distribution factor (LODF) are widely used. To the best of our knowledge, a comparative study, in terms of solution quality and computation time, for these methods has not been previously addressed. Therefore, in this paper, we summarize the solution process of these methods and compare their solution quality and computational performance through case studies on the IEEE 24-bus Reliability Test System and 118-bus system.

B. Literature Review

This section reviews the research related to the SCOPF problem and its solution methods. The studies based on the Benders decomposition method are reviewed first. References [13] and [14] gave a review of the early studies and proposed a general Benders decomposition structure for power system decision problems, including the SCOPF problem. In these studies, the contingencies in the considered contingency set are checked one by one through the so-called feasibility check subproblem. The Benders cut was generated and added to the master problem if there is a violation. However, as the number of contingency cases increases, the checking process will be very time-consuming. In this sense, robust optimization is applied to solve this problem. In the robust optimization method, a max-min bilevel subproblem [15] is used to identify the worst contingency case with the largest violation. Reference [16] proposed a two-stage robust optimization approach to solve the $N-k$ contingency-constrained unit commitment problem. Reference [17] presented an energy and reserve scheduling model with an adjustable robust optimization approach. Both generator and transmission line contingencies were considered in the above two references. In [18], the outage probabilities of the generating units are considered in the uncertainty set of $N-k$ outages to avoid a conservative solution. In [19] a robust SCUC considering load and wind uncertainty as well as generator and transmission line $N-k$ contingencies was proposed. Reference [20] investigated the distinct performance of different robust SCUC models considering the uncertainty of wind power generation. Although this paper did not consider the security constraint of contingencies, it provides a good explanation of robust optimization methods for dealing with power system uncertainty. In the above studies, either the Benders cut or column-and-constraint generation (C&CG) cutting plane was added to the master problem to eliminate the violations. Although almost all of the literature discussed above focuses on robust SCUC rather than robust SCOPF, the modeling and solution framework for contingency constraints used in these papers can also be applied to SCOPF.

In addition to Benders decomposition and robust optimization methods, the line outage distribution factor is also used for the PSCOPF problem based on DC power flow. Although the DC power flow equation does not provide explicit information on bus voltages and reactive power and has a poor accuracy in computing the active power flows on the lines with high R/X ratio, it has been extensively used in both research works and actual practice because of its high computational efficiency [21], especially when a large number of contingencies are considered in the model. Reference [22] proposed a security-constrained unit commitment in which the formulation of $N-1$ security constraint based on the LODF was used. The same idea was used in [23] and [24] to solve the resilience-constrained economic dispatch model with $N-2$ security constraints. Reference [25] proposed a refinement of the procedures presented in [22] to identify the critical subset of security constraints efficiently. However, the LODF method can only be used for PSCOPF with $N-k$ security criterion of transmission line, but not for corrective SCOPF and generator contingencies.

Although the BD, RO, and LODF methods have been widely used in the literature of the SCOPF problem or SCUC problem to deal with the contingency constraints, to the best of our knowledge, a comparative study in terms of solution quality and computation time of these methods are lacking. The computational efficiency of these methods is investigated on the IEEE 24-bus Reliability Test System and 118-bus system in this paper.

C. Main Focus and Organization

The main focus of this paper is summarized as follows.

1. Summarize the detailed solution procedures of the BD, RO, and LODF methods for solving the $N-k$ SCOPF problem. The solution quality and computational performance of these methods are investigated by the case studies on the IEEE 24-bus Reliability Test System and 118-bus system.

2. Propose a RO-PCSCOPF model in which the STL and the LTL of power flow on the branch are both taken into account. Compared with the existing RO-CSCOPF model that only considers STL or LTL, the proposed RO-PCSCOPF model can achieve a more reliable solution.

The organization of the remainder of this paper is as follows: Section II provides the mathematical formulation of the master problem and subproblem for solving the SCOPF problem. Section III introduces the proposed RO-PCSCOPF model. Section IV presents the computational performance of the BD, RO, and LODF methods for solving the SCOPF problem with the $N-k$ security criterion and the simulation results of the proposed RO-PCSCOPF model on the IEEE 24-bus RTS and 118-bus system. Section V presents the conclusions and suggests future studies.

II. MASTER PROBLEM AND SUBPROBLEM OF SCOPF

As explained in the introduction, the SCOPF problem is usually decomposed into an optimal power flow master problem for the pre-contingency state and a set of feasibility check subproblems for each contingency case. This section

presents the mathematical formulation of the master problem and the feasibility check subproblem. DC power flow is used in the model. The $N-k$ outages of the transmission lines are considered in this paper. With the linearized generation cost function, the master problem is determined as follows:

$$\mathbf{MP}:\ \min \sum_{i=1}^{NG} F_i + \sum_{b=1}^{NB} d_{\mathrm{b}} P_{\mathrm{LS},b} \tag{1}$$

$$F_i \geq F_{i,s},\ \forall i \in S_{\mathrm{G}},\ \forall s \in S_{\mathrm{S}} \tag{2}$$

$$F_{i,s} = m_{i,s} P_{\mathrm{G},i} + n_{i,s},\ \forall i \in S_{\mathrm{G}},\ \forall s \in S_{\mathrm{S}} \tag{3}$$

$$\sum_{i=1}^{NG} A_{b,i} P_{\mathrm{G},i} - \sum_{l=1}^{N} K_{b,l} P_{\mathrm{L},l} - (P_{\mathrm{D},b} - P_{\mathrm{LS},b}) = 0,\ \forall b \in \mathrm{S_B} \tag{4}$$

$$P_{\mathrm{L},l} = \frac{\theta_{s_l} - \theta_{e_l}}{x_l},\ \forall l \in \mathrm{S}_L \tag{5}$$

$$-P_{\mathrm{Lmax},l} \leq P_{\mathrm{L},l} \leq P_{\mathrm{Lmax},l},\ \forall l \in \mathrm{S}_L \tag{6}$$

$$\begin{cases} \theta_{\min,b} \leq \theta_{\mathrm{b}} \leq \theta_{\max,b},\ \forall b \in \mathrm{S_B}, b \neq \text{ref} \\ \theta_{\text{ref}} = 0 \end{cases} \tag{7}$$

$$P_{\mathrm{Gmin},i} < P_{\mathrm{G},i} < P_{\mathrm{Gmax},i},\ \forall i \in \mathrm{S_G} \tag{8}$$

$$0 \leq P_{\mathrm{LS},b} \leq P_{\mathrm{D},b},\ \forall b \in \mathrm{S_B} \tag{9}$$

where

$$n_{i,s} = a_i P_{\mathrm{G},i,s}^2 + b_i P_{\mathrm{G},i,s} + c_i - m_{i,s} P_{\mathrm{G},i,s} \quad \forall i \in S_{\mathrm{G}},\ \forall s \in S_{\mathrm{S}} \tag{10}$$

$$m_{i,s} = \frac{a_i P_{\mathrm{G},i,s}^2 + b_i P_{\mathrm{G},i,s} + c_i - a_i P_{\mathrm{G},i,s-1}^2 + b_i P_{\mathrm{G},i,s-1} + c_i}{P_{\mathrm{S},i}} \quad \forall i \in S_{\mathrm{G}},\ \forall s \in S_{\mathrm{S}} \tag{11}$$

$$\begin{cases} P_{\mathrm{G},i,s} = P_{\mathrm{Gmin},i} + s \cdot P_{\mathrm{S},i}, & \forall i \in S_{\mathrm{G}}, \forall s \in S_{\mathrm{S}} \\ P_{\mathrm{G},i,0} = P_{\mathrm{Gmin},i}, & \forall i \in S_{\mathrm{G}} \end{cases} \tag{12}$$

$$P_{\mathrm{S},i} = \frac{P_{\mathrm{Gmax},i} - P_{\mathrm{Gmin},i}}{NS},\ \forall i \in S_{\mathrm{G}} \tag{13}$$

The optimization (1) is to minimize the sum of generation cost and load shedding cost. Pre-planned load shedding is considered in the model to ensure the feasibility of the problem in case of any contingencies. The cost coefficient d_{b} is a sufficiently large value to avoid load shedding as much as possible. Constraints (2)–(9) model the system operation in the normal state, i.e., before the outage.

Once the master problem described above is solved, the optimal active power output $P_{\mathrm{G},i}^*$ and load shedding $P_{\mathrm{LS},b}^*$ will be passed to the sub-problems which will check the feasibility of the solution for each contingency. In this study, the feasibility check subproblem is formed in a well-known approach by introducing slack variables in the nodal active power balance Equation (4) and taking the summation of the slack variables which represents the security violation in the contingency state leading to the optimization objective function. Therefore, the feasibility check subproblem is formulated as follows:

$$\mathbf{SP}: \min w = \sum_{b=1}^{NB} (P_{\mathrm{b}}^+ + P_{\mathrm{b}}^-)$$

$$\sum_{i=1}^{NG} A_{b,i} P_{\mathrm{G},i}^c - \sum_{l=1}^{N} K_{b,l} P_{\mathrm{L},l}^c - (P_{\mathrm{D},b} - P_{\mathrm{LS},b}^*) + P_{\mathrm{b}}^+ - P_{\mathrm{b}}^- = 0 \quad \forall b \in \mathrm{S_B}(\delta_{\mathrm{b}}) \tag{14}$$

$$-(1 - J_l^c)\mathrm{M}_1 \leq P_{\mathrm{L},l}^c - \frac{\theta_{s_l}^c - \theta_{e_l}^c}{x_l} \leq (1 - J_l^c)\mathrm{M}_1 \quad \forall l \in \mathrm{S}_L(\gamma_l^-, \gamma_l^+) \tag{15}$$

$$-J_l^c P_{\mathrm{Lmax},l}\eta \leq P_{\mathrm{L},l}^c \leq J_l^c P_{\mathrm{Lmax},l}\eta,\ \forall l \in \mathrm{S}_L(\lambda_l^-, \lambda_l^+) \tag{16}$$

$$\begin{cases} \theta_{\min,b} \leq \theta_{\mathrm{b}}^c \leq \theta_{\max,b},\ \forall b \in \mathrm{S_B}, b \neq \text{ref}(\chi_{\mathrm{b}}^-, \chi_{\mathrm{b}}^+) \\ \theta_{\text{ref}}^c = 0(\sigma) \end{cases} \tag{17}$$

$$P_{\mathrm{Gmin},i} < P_{\mathrm{G},i}^c < P_{\mathrm{Gmax},i},\ \forall i \in \mathrm{S_G}(\beta_i^-, \beta_i^+) \tag{18}$$

$$-R_{\mathrm{D},i} \leq P_{\mathrm{G},i}^c - P_{\mathrm{G},i}^* \leq R_{\mathrm{U},i},\ \forall i \in \mathrm{S_G}(\alpha_i^-, \alpha_i^+) \tag{19}$$

$$P_{\mathrm{b}}^+ \geq 0, P_{\mathrm{b}}^- \geq 0,\ \forall b \in \mathrm{S_B} \tag{20}$$

Constraints (14)–(20) are the operational constraints of the system in the contingency state, i.e., after the outage. In this paper, we consider the $N-k$ outages of transmission lines, in which k represents the number of transmission lines that simultaneously fail. Referring to [16] and [26], a binary parameter J_l^c is introduced to model the state (failure or online) of the line in the event of a contingency. $J_l^c = 0$ represents the loss of line l in contingency c. $J_l^c = 1$ means that line l remains online in contingency c. With the use of (15) and (16), when $J_l^c = 0$ the post-contingency active power flow on line l is forced to be zero by (16), and when $J_l^c = 1$ the post-contingency power flow on line l is calculated based on the DC power flow equation. It is worth noting that the M_1 in (15) is often called the "big M" value where M_1 is large enough to make the constraint nonbinding. Note that J_l^c is an input parameter of **SP**, not an optimization variable. If the $N-k$ outages of transmission lines are considered in the problem, we have $\sum_{l=1}^{N}(1 - J_l^c) = k$.

Constraint (19) enforces the ramp-up and ramp-down limits of each generator between the normal and contingency states. If $R_{\mathrm{D},i}$ and $R_{\mathrm{U},i}$ are zero, $P_{\mathrm{G},i}^c$ will be $P_{\mathrm{G},i}^*$, and the SCOPF model described above is a PSCOPF problem. if $R_{\mathrm{D},i}$ and $R_{\mathrm{U},i}$ are not zero, the SCOPF model described above is a CSCOPF problem in which corrective generation redispatch is allowed in the contingency state to mitigate the violation.

If the security violation ω is smaller than the predefined threshold, the feasibility check is passed for the contingency case, otherwise, the subproblem is considered infeasible. The infeasibility information will be fed back to the master problem so that the newly generated master solution becomes feasible. The above feasibility check subproblem can be used in the solution methods based on BD and RO. In the BD method, contingency cases are checked one by one and the Bender cut of the infeasibility cases are fed back to the master, while in the RO method a bilevel max-min model based on this feasibility check subproblem is applied to find the worst contingency case with the largest security violation. As for the solution method based on LODF, it does not require solving the above subproblem to perform the post-contingency analysis. It calculates the post-contingency power flow by using the LODF and the pre-contingency power flow. Detailed solution procedures or flow charts for the methods mentioned above are shown in Appendix A.

III. RO-PCSCOPF WITH $N-k$ SECURITY CRITERION

This section presents the equations of the proposed RO-PCSCOPF model. The mathematical formulation of the master and subproblem for solving the SCOPF problem described in Section II is extended to become a RO-PCSCOPF problem in this section. Based on the subproblem **SP**, the bilevel Max-Min problem used in the RO to find the worst contingency can be formulated as follows:

$$\mathbf{BP}: \max_{J^c,y_l} \min_{P_{\mathrm{b}}^+,P_{\mathrm{b}}^-,P_{\mathrm{G},i}^c,P_{\mathrm{L},l}^c,\theta_{\mathrm{b}}^c} \sum_{b=1}^{NB}(P_{\mathrm{b}}^+ + P_{\mathrm{b}}^-) \tag{21}$$

$$\sum_{l\in \mathrm{S}_L}(1-J_l^c) \le k \tag{22}$$

$$J_l^c \in \{0,1\},\ \forall l \in \mathrm{S}_L \tag{23}$$

$$\sum_{l\in \mathrm{S}_L, s_l=1} y_l - \sum_{l\in \mathrm{S}_L, e_l=1} y_l = NB-1 \tag{24}$$

$$\sum_{l\in \mathrm{S}_L, s_l=b} y_l - \sum_{l\in \mathrm{S}_L, e_l=b} y_l = -1,\ \forall b \in \mathrm{S}_{\mathrm{B}}, b\neq 1 \tag{25}$$

$$-(NB+1)J_l^c \le y_l \le (NB+1)J_l^c,\ \forall l \in \mathrm{S}_L \tag{26}$$

$$\sum_{l\in S_L} J_l^c \cdot (\log(1-p_l) - \log(p_l)) + \sum_{l\in S_L}\log(p_l) \ge \log(p_{\mathrm{ct}}) \tag{27}$$

Constraints: (14)–(20)

It is worth noting that J_l^c is an optimization variable in this problem and not a parameter as it is in the **SP**. Constraint (22) enforces the number of outage lines is less than or equal to k. The single commodity flow method [27] is used in constraints (24)–(26) to guarantee that contingencies splitting the network are not considered in the model. Constraint (27) allows the model to take into account the outage probabilities of transmission lines. It represents that only contingency with a probability bigger than the given p_{ct} is included in the uncertainty set [28]. p_l is the outage probability of line l. Since the inner-level minimization problem is a linear programming problem, the bilevel model can be transferred into a single-level problem based on the strong duality theorem. The single-level equivalent is formulated as:

$$\mathbf{SEP}: \max R(\alpha,\beta,\gamma,\lambda,\delta,\chi,\sigma,\mu) \tag{28}$$

Constraints: (22)–(27)

$$\begin{aligned} &R(\alpha,\beta,\gamma,\lambda,\delta,\chi,\sigma,\mu) \\ &= \sum_{b\in \mathrm{S}_{\mathrm{B}}}((P_{\mathrm{LS},b}^* - P_{\mathrm{D},b})\delta_{\mathrm{b}} + \theta_{\min,b}\chi_{\mathrm{b}}^- - \theta_{\max,b}\chi_{\mathrm{b}}^+) \\ &+ \sum_{l\in \mathrm{S}_L}(-\mu_l^1 \mathrm{M}_1 - \mu_l^2 \mathrm{M}_1 - \mu_l^3 P_{\mathrm{Lmax},l}\eta - \mu_l^4 P_{\mathrm{Lmax},l}\eta) \\ &+ \sum_{i\in \mathrm{S}_{\mathrm{G}}}((P_{\mathrm{G},i}^* - R_{\mathrm{D},i})\alpha_i^- - (R_{\mathrm{U},i} + P_{\mathrm{G},i}^*)\alpha_i^+ \\ &+ P_{\mathrm{Gmin},i}\beta_i^- - P_{\mathrm{Gmax},i}\beta_i^+) \end{aligned} \tag{29}$$

$$\sum_{b\in \mathrm{S}_{\mathrm{B}}} K_{b,l}\delta_{\mathrm{b}} + \gamma_l^- - \gamma_l^+ + \lambda_l^- - \lambda_l^+ = 0,\ \forall l \in \mathrm{S}_L \tag{30}$$

$$\sum_{l\in \mathrm{S}_L}\frac{K_{b.l}}{x_l}(-\gamma_l^- + \gamma_l^+) + \chi_{\mathrm{b}}^- - \chi_{\mathrm{b}}^+ = 0,\ \forall b \in \mathrm{S}_{\mathrm{B}}, b \neq \text{ref} \tag{31}$$

$$\sum_{l\in \mathrm{S}_L}\frac{K_{b.l}}{x_l}(-\gamma_l^- + \gamma_l^+) + \chi_{\mathrm{b}}^- - \chi_{\mathrm{b}}^+ + \sigma = 0, b = \text{ref} \tag{31}$$

$$\alpha_i^- - \alpha_i^+ + \beta_i^- - \beta_i^+ - \sum_{b\in \mathrm{S}_{\mathrm{B}}} A_{b,i}\delta_{\mathrm{b}} \le 0,\ \forall i \in \mathrm{S}_{\mathrm{G}} \tag{32}$$

$$-1 \le \delta_{\mathrm{b}} \le 1,\ \forall b \in \mathrm{S}_{\mathrm{B}} \tag{33}$$

$$\begin{aligned} -(1-J_l^c)\mathrm{M}_2 \le \mu_l^1 \le (1-J_l^c)\mathrm{M}_2,\ \forall l \in \mathrm{S}_L \\ -J_l^c\mathrm{M}_2 + \gamma_l^- \le \mu_l^1 \le J_l^c\mathrm{M}_2 + \gamma_l^-,\ \forall l \in \mathrm{S}_L \end{aligned} \tag{34}$$

$$\begin{aligned} -(1-J_l^c)\mathrm{M}_2 \le \mu_l^2 \le (1-J_l^c)\mathrm{M}_2,\ \forall l \in \mathrm{S}_L \\ -J_l^c\mathrm{M}_2 + \gamma_l^+ \le \mu_l^2 \le \gamma_l^+ + J_l^c\mathrm{M}_2,\ \forall l \in \mathrm{S}_L \end{aligned} \tag{35}$$

$$\begin{aligned} -J_l^c\mathrm{M}_2 \le \mu_l^3 \le J_l^c\mathrm{M}_2,\ \forall l \in \mathrm{S}_L \\ -(1-J_l^c)\mathrm{M}_2 + \lambda_l^- \le \mu_l^3 \le \lambda_l^- + (1-J_l^c)\mathrm{M}_2,\ \forall l \in \mathrm{S}_L \end{aligned} \tag{36}$$

$$\begin{aligned} -J_l^c\mathrm{M}_2 \le \mu_l^4 \le J_l^c\mathrm{M}_2,\ \forall l \in \mathrm{S}_L \\ -(1-J_l^c)\mathrm{M}_2 + \lambda_l^+ \le \mu_l^4 \le \lambda_l^+ + (1-J_l^c)\mathrm{M}_2,\ \forall l \in \mathrm{S}_L \end{aligned} \tag{37}$$

$$\gamma_l^-, \gamma_l^+, \lambda_l^-, \lambda_l^+, \chi_{\mathrm{b}}^-, \chi_{\mathrm{b}}^+, \beta_i^-, \beta_i^+, \alpha_i^-, \alpha_i^+ \ge 0, \delta_{\mathrm{b}} \text{ unrestricted} \tag{38}$$

It is worth noting that the nonlinear terms in the original dual objective function due to the multiplication of the dual and integer variables J_l^c are reformulated as a set of mixed-integer linearization constraints (34)–(37) according to the Big M method [16], [29]. Since two types of post-contingency actions and operating limits are considered in the proposed RO-PCSCOPF model, we need two types of subproblem **SEP** to identify the worst contingency case for different control actions and operating limits. In the first new subproblem **SEP1** considering preventive actions and STL, the $R_{\mathrm{D},i}$ and $R_{\mathrm{U},i}$ are set to zero and η is set to be the STL.

$$\begin{aligned} &\mathbf{SEP1}: \max (29) \\ &\text{s.t. } (22)\text{–}(27),\ (30)\text{–}(38) \\ &\eta = \text{STL} \\ &R_{\mathrm{U},i} = 0, R_{\mathrm{D},i} = 0,\ \forall i \in \mathrm{S}_{\mathrm{G}} \end{aligned} \tag{39}$$

In the second new subproblem **SEP2** considering corrective actions and LTL, the $R_{\mathrm{D},i}$ and $R_{\mathrm{U},i}$ are set to the pre-defined ramping limits ΔP_i and η is set to be the LTL.

$$\begin{aligned} &\mathbf{SEP2}: \max (29) \\ &\text{s.t. } (22)\text{–}(27),\ (30)\text{–}(38) \\ &\eta = \text{LTL} \\ &R_{\mathrm{U},i} = \Delta P_i, R_{\mathrm{D},i} = \Delta P_i,\ \forall i \in \mathrm{S}_{\mathrm{G}} \end{aligned} \tag{40}$$

With the above two new subproblems, **SEP1** and **SEP2,** and the master problem **MP** the solution approach for the proposed RO-PCSCOPF model is shown in Fig. 1.

If the security violation of the found worst contingency c is larger than the predefined threshold, the BC or C&CG cutting plane for this contingency will be generated and added to the master problem until an optimal solution is found.

The infeasible Benders cut for the proposed RO-PCSCOPF problem can be formulated as follows:

$$\omega + \sum_{i=1}^{NG}(\alpha_i^- - \alpha_i^+)(P_{\mathrm{G},i} - P_{\mathrm{G},i}^*) + \sum_{b=1}^{NB}\delta_{\mathrm{b}}(P_{\mathrm{LS},b} - P_{\mathrm{LS},b}^*) \le 0 \tag{41}$$

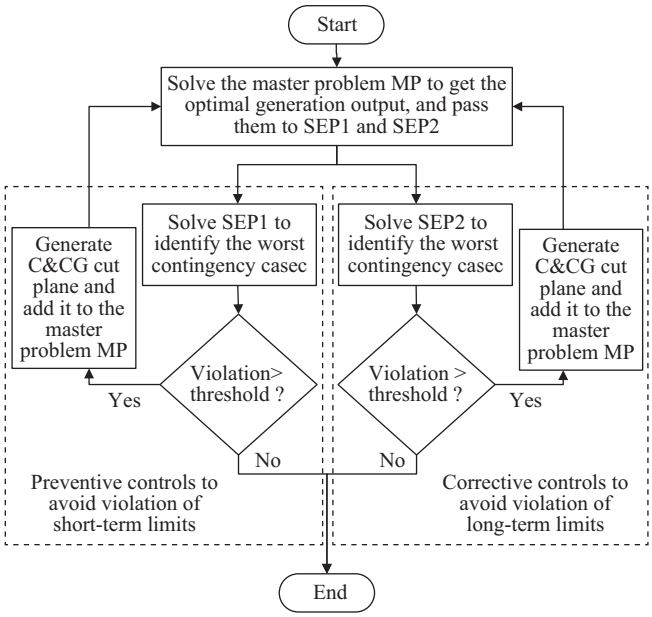

Fig. 1. Flowchart of the solution approach of the proposed RO-PCSCOPF model.

As for the C&CG cutting plane, actually, for a two-stage robust optimization problem without objective terms related to the second-stage variables, the C&CG cutting plane is a set of constraints of the second stage [30], [31], Therefore, the C&CG cutting plane for the proposed RO-PCSCOPF model is as follows:

C&CG for the worst contingency is found by **SEP1** below.

$$\sum_{i=1}^{NG} A_{b,i}P^{c}_{\mathrm{G},i} - \sum_{l=1}^{N} K_{b,l}P^{c}_{\mathrm{L},l} - (P_{\mathrm{D},b} - P_{\mathrm{LS},b}) = 0,\ \forall b \in \mathrm{S_B} \tag{42}$$

$$\eta = \mathrm{STL} \tag{43}$$

$$\text{Constraints: (15)–(20)}$$

where J^c_l is the line states determined by **SEP1**, $P^c_{\mathrm{G},i}$, $P^c_{\mathrm{L},l}$, and θ^c_{b} are a set of new variables for the identified worst contingency.

C&CG for the worst contingency is found by **SEP2** below.

$$\sum_{i=1}^{NG} A_{b,i}P^{c}_{\mathrm{G},i} - \sum_{l=1}^{N} K_{b,l}P^{c}_{\mathrm{L},l} - (P_{\mathrm{D},b} - P_{\mathrm{LS},b}) = 0,\ \forall b \in \mathrm{S_B} \tag{44}$$

$$\eta = \mathrm{LTL} \tag{45}$$

$$\text{Constraints: (15)–(20)}$$

where J^c_l is the line states determined by **SEP2**, $P^c_{\mathrm{G},i}$, $P^c_{\mathrm{L},l}$, and θ^c_{b} are a set of new variables for the identified worst contingency.

IV. Case Studies

Two case studies were conducted in this paper. The first case is to study the computational performance of the four solution methods for solving the $N-k$ SCOPF problem, i.e., the BD method, the RO-BC method, the RO-C&CG method, and the LODF method. Since LODF can only be applied to the PSCOPF problem, the PSCOPF problem with $N-k$ $(1 \le k \le 3)$ security criterion was studied to test the computational effectiveness of these four methods. The second case is to validate the reliability performance of the proposed RO-PCSCOPF model. In this case, the proposed RO-PCSCOPF model is compared with the existing RO-PSCOPF and RO-CSCOPF models.

A. Test Systems and Parameter Settings

The case studies were tested on the IEEE 24-bus RTS and 118-bus systems with system data from MATPOWER 5.0. Since MATPOWER did not provide the power flow limits of transmission lines in the IEEE 118-bus system, these data are from http://motor.ece.iit.edu/data/SCUC_118. The STL and the LTL of all lines are assumed to be 1.2 and 1, respectively. The ramp-up and ramp-down limits for each generator between normal and emergency states are set equal to 10% of the maximum output of the generator in the models considering the corrective control, that is the ΔP in **SEP2** is set to $10\%P_{\mathrm{Gmax}}$. M_1 and M_2 are set to 10,000. The convergence tolerance for all algorithms is set to 10^{-3} MWh.

All models and methods were implemented in MATLAB 2016a and YALMIP with solver Gurobi 9.1.0 on a personal computer with an Intel Core (TM) 3.20 GHz i5 processor and 8 GB of RAM. The MIP gap tolerance of Gurobi is set to 0.1%, and the other parameter is set as default. In all computational performance tests, the time limit was set to 43,200 CPU seconds (i.e., 12 h).

B. Case 1: Comparison of Different Solution Methods

1) Comparison of Computational Performance

Tables I and II summarize the computational times of the four methods for solving the PSCOPF problem with $N-k$ $(1 \le k \le 3)$ security criterion on the IEEE 24-bus RTS and 118-bus system, respectively.

The first column of Tables I and II are the security criterion and the corresponding number of contingencies of the system under such criterion. As shown in Tables I and II, there is no doubt that the classical BD method, which checks all contingencies one by one, has the slowest convergence speed. For the 24-bus RTS, this method fails to obtain the optimal

TABLE I
COMPUTATIONAL TIME OF DIFFERENT METHODS FOR SOLVING THE $N-k$ PSCOPF PROBLEM OF THE IEEE 24-BUS RTS

Methods	BD	RO-BC	RO-CCG	LODF
$N-1$ (37)	14.32 s	1.75 s	1.73 s	0.79 s
$N-2$ (659)	5287.92 s	4.60 s	4.65 s	2.45 s
$N-3$ (7503)	Timeouts	32.16 s	26.93 s	14.20 s

TABLE II
COMPUTATIONAL TIME OF DIFFERENT METHODS FOR SOLVING THE $N-k$ PSCOPF PROBLEM OF THE IEEE 118-BUS SYSTEM

Methods	BD	RO-BC	RO-C&CG	LODF
$N-1$ (177)	237.25 s	10.81 s	11.34 s	3.21 s
$N-2$ (15502)	Timeouts	143.84 s	80.77 s	75.99 s
$N-3$ (895649)	Timeouts	5641.39 s	5399.32 s	8361.86 s

solution for the $N-3$ security criterion within the time limit, while the other three methods still have a fast convergence.

As for the comparison between the RO-BC, RO-C&CG, and LODF methods, as shown in the tables, the LODF method has the best computational performance when there are not many contingencies. The convergence speed of this method slows down as the number of contingencies increases, as shown in the case of $N-3$ for the 118-bus system. This is because the LODF method is also based on the enumeration algorithm and requires the calculation of the post-contingency power flow for each contingency.

As for the comparison of the RO-BC and RO-C&CG methods, simulation results in [30] show that the convergence speed of the Benders cuts is much slower than that of the column-and-constraint generation cutting plane in most mixed-integer linear programming problems. Because Benders cuts are very weak feasibility cuts, they lead to an increase in the number of iterations between the master problem and the subproblems. However, in solving the linear SCOPF problem based on the DC power flow, these two methods have a similar computational performance in all cases, as shown in Tables I and II. The RO-C&CG method only performs a little better than the RO-BC method. This is because the master problem for solving the SCOPF problem is linear and easy to solve. Even if the number of iterations increases, the total solution time does not increase very much.

Table III shows the detailed computation results of the $N-3$ case of the 24-bus system and the 118-bus system. Fig. 2 shows the convergence curves of the RO-BC method, RO-C&CG method, and LODF method for the $N-3$ case of the 24-bus RTS and the 118-bus system.III

As shown in Fig. 2, all methods converge after a few iterations, and the LODF method requires fewer iterations, compared with the robust optimization method. This is because the LODF method generates and adds the security constraints for all violating contingencies to the master problem at each iteration, while the robust optimization method generates security constraints for only the worst contingencies. It can be seen in Table III, in the case of the IEEE 118-bus system, the total computation time to solve the subproblem is much higher than the total computation time to solve the master in the RO-BC and RO-C&CG methods. This indicates that the complexity of the master problem is acceptable. However, the bottleneck is the subproblem. One reason is that the subproblem is a mixed-integer linear programming problem, while the master problem is a linear programming problem. In particular, it is primarily due to the big-M formulation in the subproblem,

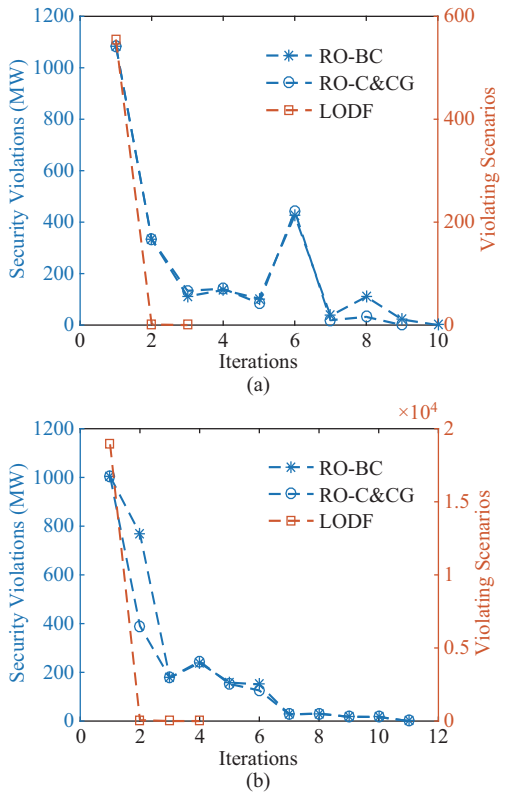

Fig. 2. The convergence curves of the RO-BC method, RO-C&CG method and LODF method for solving the $N-3$ PSCOPF problem of the 24-bus RTS and the 118-bus system.

e.g., the big-M formulation usually leads to a big optimality gap. In addition, too much redundancy/symmetry (in terms of which component to choose as a contingency) makes it difficult for the solver to determine. Acceleration techniques can be developed to improve the computational performance of the subproblem in future studies.

2) Comparison of Solution Quality

As for the solution quality, Fig. 3. shows the generation cost per iteration for the 24-bus system and the 118-bus system for the $N-3$ case. All methods achieved the same optimal solution on the IEEE 24-bus RTS. As for the case of the IEEE 118-bus system, we can see that not all methods achieve the same optimal solution. The LODF method found the lowest-cost operation. Such a result may exist because the constraints added to the master problem generated by the above methods are different. The solutions of robust optimization methods are usually overly conservative because the worst contingencies

TABLE III
THE DETAILED COMPUTATIONAL RESULTS FOR THE $N-3$ PSCOPF PROBLEM OF THE IEEE 24-BUS RTS AND THE 118-BUS SYSTEM

Systems	IEEE 24-bus Reliability Test System			IEEE 118-bus system		
Methods	RO-BC	RO-C&CG	LODF	RO-BC	RO-C&CG	LODF
Objective ($)	54,241, 118.34	54,241, 118.34	54,241, 118.34	130,621.71	130,621.71	130,480.43
Generation Cost ($)	81,608.29	81,608.29	81,608.29	130,621.71	130,621.71	130,480.43
Load Shedding (MW)	54.15	54.15	54.15	0	0	0
Total Iterations	10	9	3	11	11	4
Total Time (s)	32.16	26.93	14.20	5641.39	5399.32	8361.86
Time for MP (s)	2.63	2.63	3.59	16.85	21.49	314.51
Time for SP (s)	29.53	24.30	10.61	5624.54	5377.83	8047.35

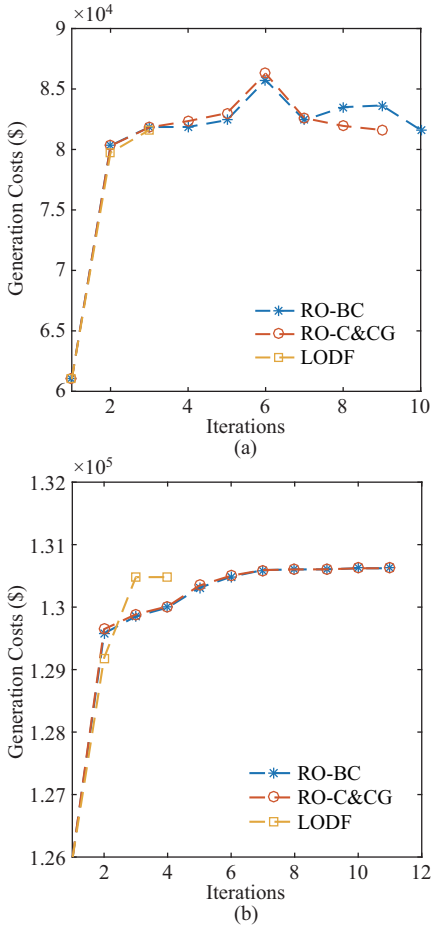

Fig. 3. Generation cost per iteration of the RO-BC method, RO-C&CG method and LODF method for solving the $N-3$ PSCOPF problem of the 24-bus RTS and the 118-bus system.

are considered in each iteration.

In addition, it can be seen in the third row of Table III that there is load shedding at the PSCOPF with $N-3$ security criterion on the IEEE 24-bus RTS. This indicates that the 24-bus RTS is not able to operate under the $N-3$ security criterion without pre-planned load shedding. In daily operations, the system must meet load demand at all times, and pre-planned load shedding is not desirable. However, these results provide system operators with valuable information about the ability of the power system to withstand multiple contingencies. In other words, the pre-planned load shedding variables considered in this study can help identify that the system is not able to be operated under such tight security criteria.

In summary, regarding the computational performance of the SCOPF problem based on DC power flow equations, the classical BD method has the worst performance, and the RO method and the LODF method have comparable performance. However, the LODF method can only be used for the PSCOPF problem and not for the CSCOPF problem. The RO method can be used for both. The bottleneck in solving the SCOPF problem is the solution of the sub-problem. In the RO method, the Big-M formulation used to linearize the bilinear terms has a greater impact on the computational efficiency. Acceleration techniques can be developed to improve the computational performance of the subproblem in future studies. Both the Bender cut and column-and-constraint generation cutting planes are used in the RO method. For the case studies in this paper, the computational performance of these two methods is not very different. The RO-C&CG method only performs a little better than the RO-BC method. As for the solution quality, in most cases, these four methods can achieve the same objective value, but in some cases, the RO method may find an over-conservative solution.

C. Case 2: Study of The Proposed RO-PCSCOPF

This case is to validate the economic and reliability performance of the proposed RO-PCSCOPF model. In this case, the proposed RO-PCSCOPF model is compared with the existing RO-PSCOPF and RO-CSCOPF models.

1) Comparison of Generation Costs and Computation Performance

Table IV shows the simulation results for the above three models with $N-1$, $N-2$, and $N-3$ safety criteria. The generation costs and load shedding, as well as the computation times for various models, are demonstrated. It can be seen that the RO-PSCOPF solution is the most conservative one. It has the highest generation cost in all cases without load shedding. This is obvious because the optimal power dispatch scheme

TABLE IV
COMPARISON OF GENERATION COST AND COMPUTATION TIME BETWEEN DIFFERENT ROBUST SCOPF MODELS OF THE IEEE 24-BUS RTS AND THE 118-BUS SYSTEM

	Systems	IEEE 24-bus Reliability Test System			IEEE 118-bus system		
	Models	RO-PSCOPF	RO-CSCOPF	RO-PCSCOPF	RO-PSCOPF	RO-CSCOPF	RO-PCSCOPF
$N-1$	Generation Costs ($)	61,001.29	61,001.29	61,001.29	127,321.10	126,738.40	126,922.03
	Reduced Cost (%)	0	0	0	0	0.5%	0.3%
	Load Shedding (MW)	0	0	0	0	0	0
	Computation Time (s)	2.33	2.35	3.69	11.22	24.52	37.13
$N-2$	Generation Costs ($)	73,127.17	68,457.96	69,407.23	128,866.48	127,208.19	128,024.15
	Reduced Costs (%)	0	6.4%	5.1%	0	1.2%	0.7%
	Load Shedding (MW)	5	5	5	0	0	0
	Computation Time (s)	7.45	13.93	14.91	93.23	80.06	437.87
$N-3$	Generation Costs ($)	81,575.18	68,789.23	84,508.21	132,069.20	129,037.35	130,621.71
	Reduced Costs (%)	0	15.7%	-3.6%	0	2.2%	1.1%
	Load Shedding (MW)	178.17	77.37	93.25	0	0	0
	Reduced Load Shedding (MW)	0	100.8	84.92	0	0	0
	Computation Time (s)	34.17	27.84	80.75	14,359.90	23,819.87	30,068.81

for the RO-PSCOPF must prevent violations of the tightening long-term limits in normal and contingency states, where expensive generators may be forced to increase their output. The high cost makes the scheduling solution the most reliable and secure solution. However, as the number of outage lines increases, RO-PSCOPF may result in the largest pre-planned load shedding, for example, in the case of RO-PSCOPF with $N-3$ security criterion on the IEEE 24-bus RTS.

The RO-CSCOPF model has the most economical solution in all cases, e.g., 15.7% reduction in generation cost and 100.8 MW reduction in load shedding compared to RO-PSCOPF in the case of $N-3$ security criterion on the IEEE 24-bus RTS. This is because CSCOPF allows for corrective generation dispatch in a post-contingency state to eliminate violations and does not consider redispatch costs in the objective function. However, if the generator is not able to quickly ramp up or down in a post-emergency state, the system may suffer a cascading blackout. This is why the RO-PCSCOPF model is proposed in this paper, which considers both preventive and corrective actions for the post-contingency state. We will analyze the security and reliability performance of the solutions for different models in the next section.

As for the proposed RO-PCSCOPF model, it can be seen that in most cases, its generation cost is between that of the RO-PSCOPF model and the RO-CSCOPF model. This is reasonable because the short-term emergency rating is larger than the long-term operational rating, resulting in a looser security constraint for the RO-PCSCOPF and therefore a cheaper solution than the RO-PSCOPF solution. But such a result is not a certainty, because RO-PCSCOPF also takes into account corrective actions, which may have some impact on the cost. Compared to the RO-CSCOPF model, the additional security constraint of short-term emergency rating is considered in the RO-PCSCOPF model, then the cost is increased.

In terms of computation time, the RO-PSCOPF model and the RO-CSCOPF model have similar computation times when the same security criterion is considered in the model. The proposed RO-PCSCOPF takes longer to converge because it must solve two subproblems to find the maximum violation of the short-term emergency limit and the long-term operating limit in each iteration, respectively.

2) Contingency Violations and Reliability Analysis

As mentioned above, the power dispatch solution of the RO-PSCOPF model is the most expensive but reliable, with no violations in the post-emergency state. In this section, the reliability of solutions of the RO-CSCOPF model and the RO-PCSCOPF model are analyzed. Table V shows the number of violating contingency and the maximum violations for these two models on the IEEE 24-bus RTS and 118-bus system.

NVS and NVL are the numbers of contingencies that result in violations of the short-term emergency limit and the long-term operating limit, respectively, if corrective actions are not taken after the occurrence of a contingency. MVS and MVL are the maximum violations of the short-term emergency limit and the long-term operating limit, respectively. As shown in the table, there is no doubt that the NVS of the RO-PCSCOPF model is equal to zero because the short-term emergency limit has been taken into account in the optimization model.

TABLE V
NUMBER OF VIOLATING CONTINGENCY AND MAXIMUM VIOLATIONS OF THE RO-CSCOPF MODEL AND THE PROPOSED RO-PCSCOPF MODEL OF THE IEEE 24-BUS RTS AND THE 118-BUS SYSTEM

Systems		IEEE 24-bus RTS		IEEE 118-bus system	
Models		RO-CSCOPF	RO-PCSCOPF	RO-CSCOPF	RO-PCSCOPF
$N-1$	NVS	0	0	2	0
	MVS (MW)	0	0	45	0
	NVL	0	0	3	3
	MVL (MW)	0	0	115	82.57
$N-2$	NVS	4	0	179	0
	MVS (MW)	70	0	156.25	0
	NVL	15	7	180	178
	MVL (MW)	230	200	237.72	81.46
$N-3$	NVS	157	0	Timeouts	0
	MVS (MW)	697	0	226.14	0
	NVL	266	20	Timeouts	Timeouts
	MVL (MW)	857	198.68	320.52	103.38

In terms of NVL and MVL, for the 118-bus system, even under the $N-1$ security criterion, the RO-CSCOPF model has 3 contingencies that result in a violation of the long-term operating limit, with a maximum violation of 115 MW (outage of line 8). In general, the NVL and MVL of the RO-PCSCOPF model are smaller than those of the RO-CSCOPF model. For example, in the $N-3$ case of 24-bus RTS, the NVL of the RO-PCSCOPF model is only 20, while it is 266 in the RO-CSCOPF model. For some cases, for example, in the $N-1$ case of the 118-bus system, the RO-CSCOPF model and the RO-PCSCOPF model have the same NVL, but the RO-PCSCOPF model has a smaller maximum violation amount. The above results suggest that the power dispatch solution of the proposed RO-PCSCOPF model not only ensures that short-term limits are not violated but also reduces violations of long-term limits in a post-contingency state.

As for the NVS of the RO-CSCOF model, we can see that for the 118-bus system, even under the $N-1$ security criterion, the RO-CSCOPF model has 2 contingencies that result in a violation of the short-term operating limit, with a maximum violation of 45 MW and the 24-bus RTS has 4 and 157 violating contingencies of $N-2$ and $N-3$ security criterion, respectively. If corrective action is not quickly taken, longer violations of short-term limits could lead to continued outages. We then consider the example of the outage of lines 23 and 29 on the IEEE 24-bus RTS. The active power output of the generators on the IEEE 24-bus RTS obtained from the RO-PSCOPF model, the RO-CSCOPF, and the proposed RO-PCSCOPF model are shown in Fig. 4. In the proposed model, most of the generators have a similar generation dispatch solution to that of the RO-CSCOPF model while some have different solutions, such as generators 11, 12, and 13. The power output of some generators is closer to that of the RO-PCSCOPF, which is adjusted to avoid security violations of the STL. Fig. 5 shows the pre-contingency and post-contingency power flows on transmission lines of this power dispatch solution under the $N-2$ contingency of lines 23 and 29.

As shown in Fig. 5, the pre-contingency and post-contingency power flow of the RO-PSCOPF model are all under the LTL as expected. In the RO-CSCOPF model, the power flows of lines 6 and 7 are over the STL, as shown in

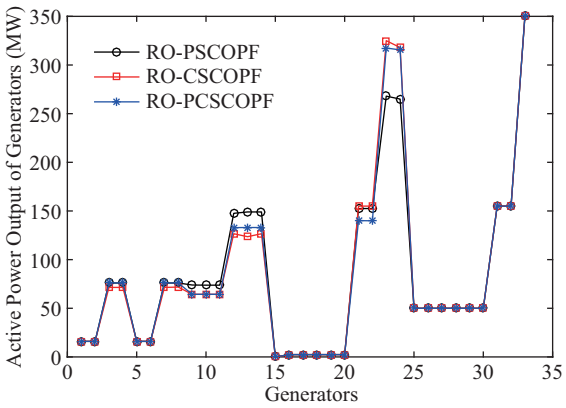

Fig. 4. The active power output of the generators on the IEEE 24-bus under the $N-2$ security criterion.

the second graph in Fig. 5. The violation could be removed by corrective generation dispatch, as shown in the third graph. However, if the generator can not ramp up or down very quickly, lines 6 and 7 may be on outage due to overload. If lines 6 and 7 are out of service, load levels on lines 28 and 29 will increase to 1.55 and 1.52 p.u. These two lines may continue to fail. This may develop into a cascading outage blackout. However, in the RO-PCSCOPF model, preventive control is used to limit the power flow in lines 6 and 7 below the short-term limit to avoid overload.

In summary, compared to the RO-PSCOPF model, in the proposed RO-PCSCOPF, corrective control is allowed to respond to a contingency. Therefore, the operating cost is reduced to some extent. In the RO-CSCOPF model, contingencies may cause some branch flows to exceed not only their long-term operating limit but also the short-term emergency limit. Ignoring such violations may result in cascading outages. The power dispatch scheme of the proposed RO-PCSCOPF model is more reliable if corrective controls are not implemented in a short time.

V. Conclusion

In this paper, the computational efficiency and solution quality of the BD, RO, and LODF methods for solving the SCOPF problem based on DC power flow are investigated on the IEEE 24-bus Reliability Test System and 118-bus system. Simulation results show that the classical BD method has the worst performance, and the RO method and the LODF method have comparable performance. However, the LODF method can only be used for the PSCOPF problem and not for the CSCOPF problem. The RO method can be used for both. For the comparison between BC and C&CG, the RO-C&CG method only performs a little better than the RO-BC method. As for the solution quality, in most cases, these four methods could achieve similar results, but in some cases, the RO method may find an over-conservative solution. Based on the comparison study, a RO-PCSCOPF model is proposed. The short-term emergency limit and long-term operating limit of power flow on the branch in the post-contingency state are both taken into account in the problem. Compared to the RO-PSCOPF model, in the proposed RO-PCSCOPF model, corrective control is allowed to respond to a contingency. Therefore, the operating cost is reduced to some extent. Compared with the existing RO-CSCOPF model that only considers the short-term emergency limit or the long-term operating limit, the proposed RO-PCSCOPF model can achieve a more reliable solution. In a future study, RO-PCSCOPF based on AC power flow will be investigated. Uncertainty of renewable energy generation and energy storage systems for quick response will also be studied.

Appendix

A. Flowchart of The BD Method for Solving The SCOPF Problem

With master problem **MP** and subproblem **SP** described in Section II, the flowchart of the BD method for solving the SCOPF problem is shown in Fig. A1. If the security violation of contingency c is larger than the predefined threshold, the Benders cut for this contingency will be generated and added to the master problem. Mathematically, Benders cut is the first-order approximation of the objective function of the feasibility check problem around the point determined by the master problem. The sense of this cut is to force the objective value of the feasibility check problem to be less than or equal to

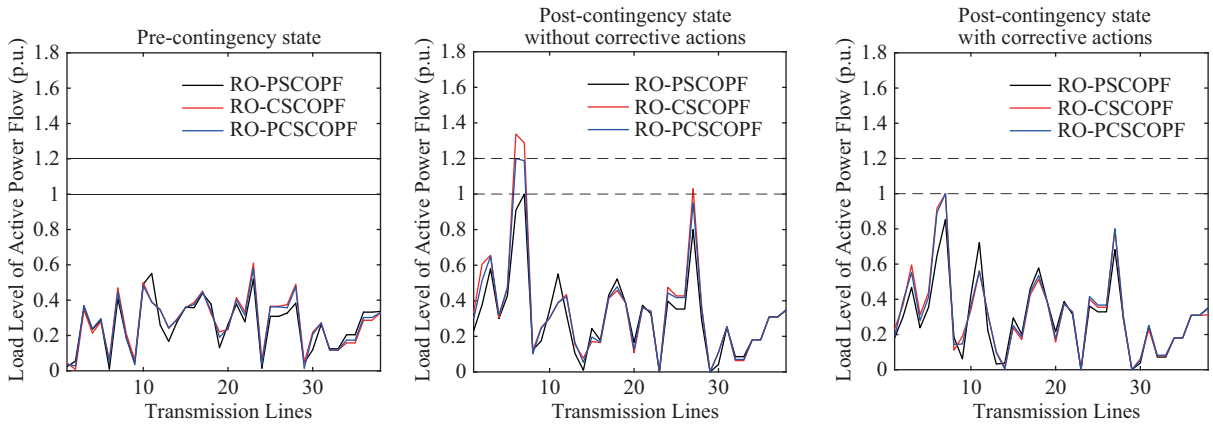

Fig. 5. Pre-contingency and post-contingency power flow on the transmission lines of the IEEE 24-bus RTS under $N-2$ contingency of lines 23 and 29.

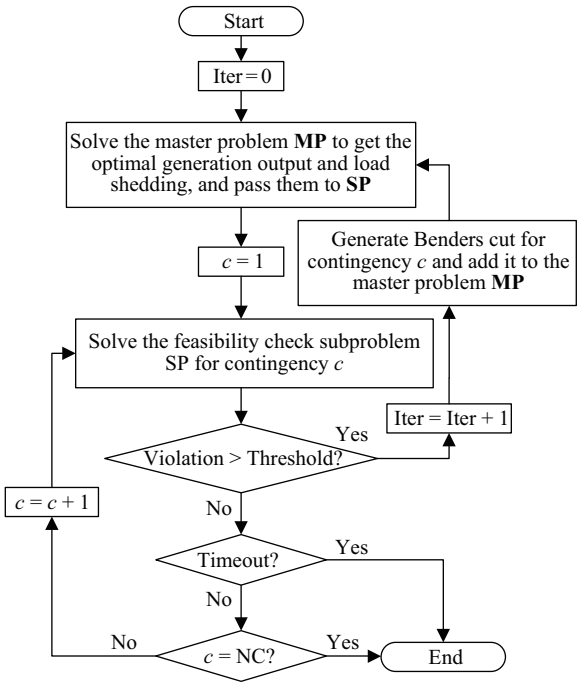

Fig. A1. Flowchart of the BD method for solving the SCOPF problem.

zero in the next iteration, therefore, making the subproblem feasible. The Benders cut for the SCOPF problem described in Section II can be formulated as follows:

$$\omega+\sum_{i=1}^{NG}(\alpha_i^- -\alpha_i^+)(P_{\mathrm{G},i}-P_{\mathrm{G},i}^*)+\sum_{b=1}^{NB}\delta_{\mathrm{b}}(P_{\mathrm{LS},b}-P_{\mathrm{LS},b}^*)\le 0 \tag{46}$$

In (46), α_i^-, α_i^+ and δ_{b} are dual variables for constraints (19) and (14), respectively, which can be obtained from the dual function of the solver or by the dual problem **AP1** as follows:

$$\mathbf{AP1}: \max G(\alpha,\beta,\gamma,\lambda,\delta,\chi,\sigma) \tag{47}$$

$$\begin{aligned}&G(\alpha,\beta,\gamma,\lambda,\delta,\chi,\sigma)\\&=\sum_{b\in \mathrm{S_B}}(-(P_{\mathrm{D},b}-P_{\mathrm{LS},b}^*)\delta_{\mathrm{b}}+\theta_{\min,b}\chi_{\mathrm{b}}^- -\theta_{\max,b}\chi_{\mathrm{b}}^+)\\&\quad+\sum_{l\in \mathrm{S}_L}(-\gamma_l^-(1-J_l^c)\mathrm{M}_1-\gamma_l^+(1-J_l^c)\mathrm{M}_1)\\&\quad+\sum_{l\in \mathrm{S}_L}(-\lambda_l^- P_{\mathrm{Lmax},l}\eta-\lambda_l^+ P_{\mathrm{Lmax},l}\eta)\\&\quad+\sum_{i\in \mathrm{S_G}}(-(R_{\mathrm{D},i}-P_{\mathrm{G},i}^*)\alpha_i^- -(R_{\mathrm{U},i}+P_{\mathrm{G},i}^*)\alpha_i^+)\\&\quad+\sum_{i\in \mathrm{S_G}}(P_{\mathrm{Gmin},i}\beta_i^- -P_{\mathrm{Gmax},i}\beta_i^+)\end{aligned} \tag{48}$$

$$\sum_{b\in \mathrm{S_B}}K_{b,l}\delta_{\mathrm{b}}+\gamma_l^- -\gamma_l^+ +\lambda_l^- -\lambda_l^+ =0,\ \forall l\in \mathrm{S}_L \tag{49}$$

$$\sum_{l\in \mathrm{S}_L}\frac{K_{b.l}}{x_l}(-\gamma_l^- +\gamma_l^+)+\chi_{\mathrm{b}}^- -\chi_{\mathrm{b}}^+ =0,\ \forall b\in \mathrm{S_B}, b\ne \mathrm{ref}$$

$$\sum_{l\in \mathrm{S}_L}\frac{K_{b.l}}{x_l}(-\gamma_l^- +\gamma_l^+)+\chi_{\mathrm{b}}^- -\chi_{\mathrm{b}}^+ +\sigma=0, b=\mathrm{ref} \tag{50}$$

$$\alpha_i^- -\alpha_i^+ +\beta_i^- -\beta_i^+ -\sum_{b\in \mathrm{S_B}}A_{b,i}\delta_{\mathrm{b}}\le 0,\ \forall i\in \mathrm{S_G} \tag{51}$$

$$-1\le \delta_{\mathrm{b}}\le 1,\ \forall b\in \mathrm{S_B} \tag{52}$$

$$\gamma_l^-,\gamma_l^+,\lambda_l^-,\lambda_l^+,\chi_{\mathrm{b}}^-,\chi_{\mathrm{b}}^+,\beta_i^-,\beta_i^+,\alpha_i^-,\alpha_i^+\ge 0,\delta_{\mathrm{b}}\ \text{unrestricted} \tag{53}$$

B. Flowchart of The RO-BD and RO-CCG Methods for Solving The SCOPF Problem

With master problem **MP** and subproblem **SEP** described in Section II, the flowchart of the RO-BD and RO-CCG methods for solving the SCOPF problem is shown in Fig. B1.

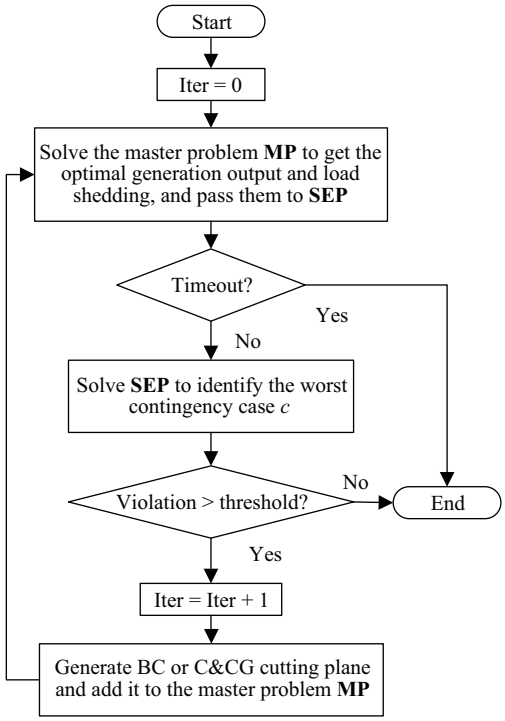

Fig. B1. Flowchart of the robust optimization method for solving the SCOPF problem.

As shown in Fig. B1, if the security violation of the found worst contingency c is larger than the predefined threshold, the BC or C&CG cutting plane for this contingency will be generated and added to the master problem **MP**. It is worth noting that the Benders cut explained in the BD method can also be used here. As for the C&CG cutting plane, actually, for a two-stage robust optimization problem without objective terms related to the second-stage variables, the C&CG cutting plane is a set of constraints of the second stage [30]. Therefore, the C&CG cutting plane for RO-SCOPF is as follows:

$$\sum_{i=1}^{NG}A_{b,i}P_{\mathrm{G},i}^c-\sum_{l=1}^{N}K_{b,l}P_{\mathrm{L},l}^c-(P_{\mathrm{D},b}-P_{\mathrm{LS},b})=0,\ \forall b\in \mathrm{S_B}$$

$$-(1-J_l^c)\mathrm{M}_1\le P_{\mathrm{L},l}^c-\frac{\theta_{s_l}^c-\theta_{e_l}^c}{x_l}\le(1-J_l^c)\mathrm{M}_1,\ \forall l\in \mathrm{S}_L$$

$$-J_l^c P_{\mathrm{Lmax},l}\eta\le P_{\mathrm{L},l}^c\le J_l^c P_{\mathrm{Lmax},l}\eta,\ \forall l\in \mathrm{S}_L$$

$$\theta_{\min,b}\le\theta_{\mathrm{b}}^c\le\theta_{\max,b},\ \forall b\in \mathrm{S_B}, b\ne \mathrm{ref}$$

$$\theta_{\mathrm{ref}}^c=0$$

$$P_{\mathrm{Gmin},i}<P_{\mathrm{G},i}^c<P_{\mathrm{Gmax},i},\ \forall i\in \mathrm{S_G}$$

$$-R_{\mathrm{D},i} \le P^c_{\mathrm{G},i} - P_{\mathrm{G},i} \le R_{\mathrm{U},i},\ \forall i \in \mathrm{S_G} \tag{54}$$

where J^c_l is the line states determined by **SEP**, $P^c_{\mathrm{G},i}$, $P^c_{\mathrm{L},l}$, and θ^c_{b} are a set of new variables for the identified worst dase contingency. The C&CG is added to the master problem until an optimal solution is found.

C. Flowchart of The LODF Method for Solving The SCOPF Problem

According to the iterative contingency filtering process proposed in [22] and [23], the flowchart of the LODF method for solving the SCOPF problem is shown in Fig. C1 below.

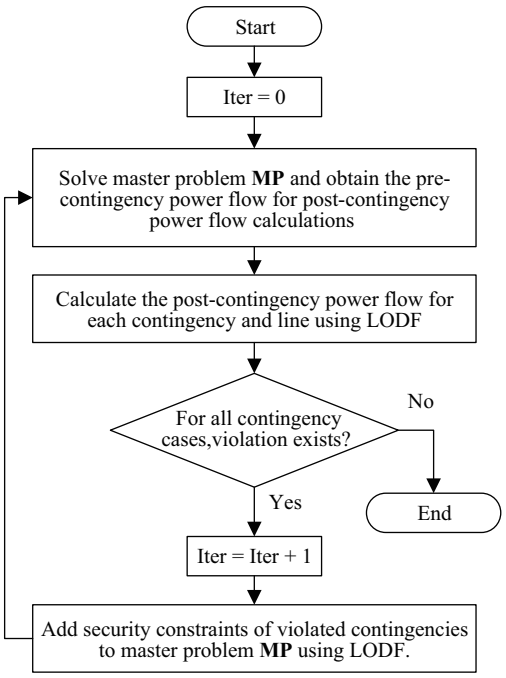

Fig. C1. Flowchart of the LODF method for solving the PSCOPF problem.

As shown in Fig. C1, in the LODF method, the post-contingency security analysis is performed by calculating the post-contingency power flow of the remaining online lines using the LODF, not by a feasibility check subproblem. The LODF is defined as the incremental active power flow on monitored lines caused by the lines on outage with a pre-contingency active power flow of one unit. LODF under a single-line outage or multi-line outage can be generalized by using the power transfer distribution factor (PTDF) of a pre-contingency network with the following equations [32].

$$\mathrm{LODF} = \mathrm{PTDF}^0_{\mathrm{M,O}}(\mathrm{E} - \mathrm{PTDF}^0_{\mathrm{O,O}})^{-1} \tag{55}$$

$$\mathrm{PTDF}^0_{\mathrm{M,O}} = \mathrm{X}^{-1}_{\mathrm{M}}\Phi^{\mathrm{T}}\mathrm{B}^{-1}\Psi \tag{56}$$

$$\mathrm{PTDF}^0_{\mathrm{O,O}} = \mathrm{X}^{-1}_{\mathrm{O}}\Psi^{\mathrm{T}}\mathrm{B}^{-1}\Psi \tag{57}$$

$$\mathrm{B}^{-1} = \mathrm{T}^{\mathrm{T}}(\mathrm{TBT}^{\mathrm{T}})^{-1}\mathrm{T} \tag{58}$$

$$\mathrm{B} = \mathrm{KX}^{-1}\mathrm{K}^{\mathrm{T}} \tag{59}$$

where LODF is a line outage distribution factor matrix with the size of $(N_{\mathrm{M}} \times N_{\mathrm{O}})$. $\mathrm{PTDF}^0_{M,O}$ and $\mathrm{PTDF}^0_{\mathrm{O,O}}$ are power transfer distribution factor matrices with the size of $(N_{\mathrm{M}} \times N_{\mathrm{O}})$ and $(N_{\mathrm{O}} \times N_{\mathrm{O}})$, respectively. E is an identity matrix with the size of $(N_{\mathrm{O}} \times N_{\mathrm{O}})$. $\mathrm{X_M}$ and $\mathrm{X_O}$ are diagonal matrices with elements representing the reactance of monitored lines and failure lines with the size of $(N_{\mathrm{M}} \times N_{\mathrm{M}})$ and $(N_{\mathrm{O}} \times N_{\mathrm{O}})$, respectively. Φ and Ψ are bus to monitored lines and bus to outage lines incidence matrices with the size of $(NB \times N_{\mathrm{M}})$ and $(NB \times N_{\mathrm{O}})$, respectively. N_{M} and N_{O} are the number of monitored lines and outage lines in a contingency. X is a diagonal matrix with elements representing the reactance of all lines with the size of $(N \times N)$. K is a bus-lines incidence matrix with the size of $(NB \times N)$. T is a reduced identity matrix with the size of $[(NB-1) \times NB]$.

After obtaining the LODF and the pre-contingency power flow $P_{\mathrm{L},l}$ from the master problem **MP**, we can calculate the post-contingency power flow of the remaining online line in a contingency. For example, for an $N-2$ contingency of lines u and v, the following equations can be used to calculate the post-contingency power flow of any remaining line l.

$$\hat{P}^c_{\mathrm{L},l,uv} = P_{\mathrm{L},l} + \mathrm{LODF}_{l,uv,u} \times P_{\mathrm{L},u} + \mathrm{LODF}_{l,uv,v} \times P_{\mathrm{L},v} \tag{60}$$

After obtaining the post-contingency power flow, check if there are any power flow violations in all contingency cases and all remaining online lines. If not, stop, otherwise, save violated contingency scenarios, and then add security constraints of these scenarios to the master problem. For example, in the contingency of lines u and v, the post contingency of line l is larger than the considered post-contingency power flow limit. Lines u, v and l will form a violated contingency scenario. The security constraint (61) of this violated contingency scenario will be added to the master problem **MP.**

$$P^c_{\mathrm{L},l,uv} = P_{\mathrm{L},l} + \mathrm{LODF}_{l,uv,u} \times P_{\mathrm{L},u} + \mathrm{LODF}_{l,uv,v} \times P_{\mathrm{L},v} \tag{61}$$

Resolve the master problem with the security constraint (61) to update the power dispatch solution, until no violated contingency scenario exists.

REFERENCES

[1] A. Monticelli, M. V. F. Pereira, and S. Granville, "Security-constrained optimal power flow with post-contingency corrective rescheduling," *IEEE Transactions on Power Systems*, vol. 2, no. 1, pp. 175–180, Feb. 1987.

[2] F. Capitanescu, J. L. Martinez Ramos, P. Panciatici, D. Kirschen, A. Marano Marcolini, L. Platbrood, and L. Wehenkel, "State-of-the-art, challenges, and future trends in security constrained optimal power flow," *Electric Power Systems Research*, vol. 81, no. 8, pp. 1731–1741, Aug. 2011.

[3] S. Frank and S. Rebennack, "An introduction to optimal power flow: theory, formulation, and examples," *IIE Transactions*, vol. 48, no. 12, pp. 1172–1197, Aug. 2016.

[4] F. Capitanescu, M. Glavic, D. Ernst, and L. Wehenkel, "Contingency filtering techniques for preventive security-constrained optimal power flow," *IEEE Transactions on Power Systems*, vol. 22, no. 4, pp. 1690–1697, Nov. 2007.

[5] F. Capitanescu and L. Wehenkel, "A new iterative approach to the corrective security-constrained optimal power flow problem," *IEEE Transactions on Power Systems*, vol. 23, no. 4, pp. 1533–1541, Nov. 2008.

[6] Y. Xu, Z. Y. Dong, R. Zhang, K. P. Wong, and M. Y. Lai, "Solving preventive-corrective SCOPF by a hybrid computational strategy," *IEEE Transactions on Power Systems*, vol. 29, no. 3, pp. 1345–1355, May 2014.

[7] Y. Xu, H. M. Yang, R. Zhang, Z. Y. Dong, M. Y. Lai, and K. P. Wong, "A contingency partitioning approach for preventive-corrective security-constrained optimal power flow computation," *Electric Power Systems Research*, vol. 132, pp. 132–140, Mar. 2016.

[8] H. Sharifzadeh and N. Amjady, "Stochastic security-constrained optimal power flow incorporating preventive and corrective actions," *International Transactions on Electrical Energy Systems*, vol. 26, no. 11, pp. 2337–2352, Nov. 2016.

[9] Y. F. Wen, C. X. Guo, D. S. Kirschen, and S. F. Dong, "Enhanced security-constrained OPF with distributed battery energy storage," *IEEE Transactions on Power Systems*, vol. 30, no. 1, pp. 98–108, Jan. 2015.

[10] Y. F. Wen, C. X. Guo, H. Pandžić, and D. S. Kirschen, "Enhanced security-constrained unit commitment with emerging utility-scale energy storage," *IEEE Transactions on Power Systems*, vol. 31, no. 1, pp. 652–662, Jan. 2016.

[11] M. A. Ortega-Vazquez, "Assessment of $N - k$ contingencies in a probabilistic security-constrained optimal power flow," in *Proceedings of 2016 IEEE Power and Energy Society General Meeting* (*PESGM*), Boston, MA, USA, 2016, pp. 1–5.

[12] X. Wu, A. J. Conejo, and N. Amjady, "Robust security constrained ACOPF via conic programming: identifying the worst contingencies," *IEEE Transactions on Power Systems*, vol. 33, no. 6, pp. 5884–5891, Nov. 2018.

[13] Y. Li and J. D. McCalley, "A general benders decomposition structure for power system decision problems," in *Proceedings of 2008 IEEE International Conference on Electro/Information Technology*, Ames, IA, USA, 2008, pp. 72–77.

[14] S. Cvijic and J. J. Xiong, "Security constrained unit commitment and economic dispatch through benders decomposition: a comparative study," in *Proceedings of 2011 IEEE Power and Energy Society General Meeting*, Detroit, MI, USA, 2011, pp. 1–8.

[15] J. M. Arroyo, "Bilevel programming applied to power system vulnerability analysis under multiple contingencies," *IET Generation, Transmission & Distribution*, vol. 4, no. 2, pp. 178–190, Feb. 2010.

[16] Q. F. Wang, J. P. Watson, and Y. P. Guan, "Two-stage robust optimization for $N - k$ contingency-constrained unit commitment," *IEEE Transactions on Power Systems*, vol. 28, no. 3, pp. 2366–2375, Aug. 2013.

[17] A. Street, A. Moreira, and J. M. Arroyo, "Energy and reserve scheduling under a joint generation and transmission security criterion: an adjustable robust optimization approach," *IEEE Transactions on Power Systems*, vol. 29, no. 1, pp. 3–14, Jan. 2014.

[18] J. Jeong and S. Park, "A robust contingency-constrained unit commitment with an $N - \alpha k$ security criterion," *International Journal of Electrical Power & Energy Systems*, vol. 123, pp. 106148, Dec. 2020.

[19] B. Q. Hu and L. Wu, "Robust SCUC considering continuous/discrete uncertainties and quick-start units: a two-stage robust optimization with mixed-integer recourse," *IEEE Transactions on Power Systems*, vol. 31, no. 2, pp. 1407–1419, Mar. 2016.

[20] B. Q. Hu, L. Wu, X. H. Guan, F. Gao, and Q. Z. Zhai, "Comparison of variant robust SCUC models for operational security and economics of power systems under uncertainty," *Electric Power Systems Research*, vol. 133, pp. 121–131, Apr. 2016.

[21] Y. Fu, Z. Y. Li, and L. Wu, "Modeling and solution of the large-scale security-constrained unit commitment," *IEEE Transactions on Power Systems*, vol. 28, no. 4, pp. 3524–3533, Nov. 2013.

[22] D. A. Tejada-Arango, P. Sánchez-Martın, and A. Ramos, "Security constrained unit commitment using line outage distribution factors," *IEEE Transactions on Power Systems*, vol. 33, no. 1, pp. 329–337, Jan. 2018.

[23] Y. F. Wang, L. P. Huang, M. Shahidehpour, L. L. Lai, and Y. Zhou, "Impact of cascading and common-cause outages on resilience-constrained optimal economic operation of power systems," *IEEE Transactions on Smart Grid*, vol. 11, no. 1, pp. 590–601, Jan. 2020.

[24] L. P. Huang, Z. X. Huang, C. S. Lai, G. Y. Yang, Z. L. Zhao, N. Tong, X. M. Wu, and L. L. Lai, "Augmented power dispatch for resilient operation through controllable series compensation and $N - 1$–1 contingency assessment," *Energies*, vol. 14, no. 16, pp. 4756, Aug. 2021.

[25] Á. S. Xavier, F. Qiu, F. Y. Wang, and P. R. Thimmapuram, "Transmission constraint filtering in large-scale security-constrained unit commitment," *IEEE Transactions on Power Systems*, vol. 34, no. 3, pp. 2457–2460, May 2019.

[26] M. Y. Yan, Y. B. He, M. Shahidehpour, X. M. Ai, Z. Y. Li, and J. Y. Wen, "Coordinated regional-district operation of integrated energy systems for resilience enhancement in natural disasters," *IEEE Transactions on Smart Grid*, vol. 10, no. 5, pp. 4881–4892, Sep. 2019.

[27] Z. Y. Li, M. Shahidehpour, A. Alabdulwahab, and A. Abusorrah, "Bilevel model for analyzing coordinated cyber-physical attacks on power systems," *IEEE Transactions on Smart Grid*, vol. 7, no. 5, pp. 2260–2272, Sep. 2016.

[28] Y. B. Chen, Z. Zhang, Z. Y. Liu, P. Zhang, Q. Ding, X. Y. Liu, and W. R. Wang, "Robust $N - -k$ CCUC model considering the fault outage probability of units and transmission lines," *IET Generation, Transmission & Distribution*, vol. 13, no. 17, pp. 3782–3791, Sep. 2019.

[29] M. Y. Yan, M. Shahidehpour, A. Paaso, L. X. Zhang, A. Alabdulwahab, and A. Abusorrah, "Distribution network-constrained optimization of peer-to-peer transactive energy trading among multi-microgrids," *IEEE Transactions on Smart Grid*, vol. 12, no. 2, pp. 1033–1047, Mar. 2021, doi: 10.1109/TSG.2020.3032889.

[30] B. Zeng and L. Zhao, "Solving two-stage robust optimization problems using a column-and-constraint generation method," *Operations Research Letters*, vol. 41, no. 5, pp. 457–461, Sep. 2013.

[31] M. Y. Yan, X. M. Ai, M. Shahidehpour, Z. Y. Li, J. Y. Wen, S. Bahramira, and A. Paaso, "Enhancing the transmission grid resilience in ice storms by optimal coordination of power system schedule with pre-positioning and routing of mobile DC de-icing devices," *IEEE Transactions on Power Systems*, vol. 34, no. 4, pp. 2663–2674, Jul. 2019.

[32] J. C. Guo, Y. Fu, Z. Y. Li, and M. Shahidehpour, "Direct calculation of line outage distribution factors," *IEEE Transactions on Power Systems*, vol. 24, no. 3, pp. 1633–1634, Aug. 2009.

Liping Huang (S'16) received the B.S. degree from China University of Mining and Technology, Beijing, China, in 2016. She is currently pursuing the Ph.D. degree with the School of Automation, Guangdong University of Technology, Guangzhou, China. She was a visiting Ph.D. student with the Center for Electric Power and Energy, Department of Electrical Engineering, Technical University of Denmark, from 2019 to 2020. Her research interests are in power system optimal operation and control, reliability, and resilience evaluation.

Chun Sing Lai (S'11–M'19–SM'20) received the B.Eng. (First Class Hons.) in electrical and electronic engineering from Brunel University London, London, UK, in 2013, and the D.Phil. degree in Engineering Science from the University of Oxford, Oxford, UK, in 2019. He is currently a Lecturer with the Department of Electronic and Electrical Engineering, Brunel University London. From 2018 to 2020, he was an UK Engineering and Physical Sciences Research Council Research Fellow with the School of Civil Engineering, University of Leeds, Leeds, UK. His current research interests are in power system optimization and data analytics. Dr. Lai was the Publications Co-Chair for both 2020 and 2021 IEEE International Smart Cities Conferences. He is the Vice-Chair of the IEEE Smart Cities Publications Committee and Associate Editor for IET Energy Conversion and Economics. He is the Working Group Chair for IEEE P2814 Standard, and the Chair of the IEEE SMC Intelligent Power and Energy Systems Technical Committee. He is an IET Member and a Chartered Engineer.

Zhuoli Zhao (S'15–M'18) received a B.S. degree and a Ph.D. degree from South China University of Technology, Guangzhou, China, in 2010 and 2017, respectively. From October 2014 to December 2015, he was a Joint Ph.D. Student (Sponsored Researcher) with the Control and Power Research Group, Department of Electrical and Electronic Engineering, Imperial College London, London, U.K. He was a Research Associate with the Smart Grid Research Laboratory, Electric Power Research Institute, China Southern Power Grid, Guangzhou, China, from 2017 to 2018. He is currently an Associate Professor with the School of Automation, Guangdong University of Technology, Guangzhou, China. His research interests include microgrid control and energy management, power electronic converters, smart grids, and distributed generation systems. He is an Active Reviewer for the IEEE Transactions on Power Electronics, the IEEE Transactions on Smart Grid, the IEEE Transactions on Sustainable Energy, the IEEE Transactions on Industrial Electronics, and the Applied Energy.

Guangya Yang received a Ph.D. in 2008 from the University of Queensland, Australia, in the field of Electrical Power Systems. Currently he is a Senior Power System Engineer with Ørsted and a Senior Scientist with Technical University of Denmark. His research focuses on power system dynamic security and protection, offshore wind power system design and control, and transactive energy applied to distributed energy resources. Since 2009, he has been developing and leading many industrial collaborative projects in Denmark. He is an editorial board member of IEEE Transactions on Sustainable Energy, IEEE Transactions on Power Delivery, IEEE Access, and Journal of Modern Power System and Clean Energy.

Bang Zhong received a B.S. degree from Hunan Institute of Engineering, Xiangtan, China, in 2013, a M.S. degree from Guangdong University of Technology, Guangzhou, China, in 2017. He is currently an engineer at Zhaoqing Power Supply Bureau, Guangdong Power Grid Company, China Southern Power Grid.

Loi Lei Lai received B.Sc. (First Class Hons.), Ph.D., and D.Sc. degrees in Electrical and Electronic Engineering from the University of Aston, Birmingham, UK, and City, University of London, London, UK, in 1980, 1984, and 2005, respectively. Professor Lai is currently a University Distinguished Professor with Guangdong University of Technology, Guangzhou, China. He was a Pao Yue Kong Chair Professor with Zhejiang University, Hangzhou, China, and the Professor and Chair of Electrical Engineering with City, University of London. His current research areas are in smart cities and smart grid. Professor Lai is an Associate Editor of the IEEE Transactions on Systems, Man, and Cybernetics: Systems, Editor-in-Chief of the IEEE Smart Cities Newsletter, a member of the IEEE Smart Cities Steering Committee and the Chair of the IEEE Systems, Man, and Cybernetics Society (IEEE/SMCS) Standards Committee. He was a member of the IEEE Smart Grid Steering Committee; the Director of Research and Development Center, State Grid Energy Research Institute, China; a Vice President for Membership and Student Activities with IEEE/SMCS; and a Fellow Committee Evaluator for the IEEE Industrial Electronics Society. He is a Fellow of IET.